Thermodynamics of micelle formation of the ephedrine-based chiral cationic surfactant DMEB in water, and the intercalation of DMEB in montmorillonite

ARTICLE *in* COLLOIDS AND SURFACES A PHYSICOCHEMICAL AND ENGINEERING ASPECTS · APRIL 2008

Impact Factor: 2.75 · DOI: 10.1016/j.colsurfa.2007.06.056

4 AUTHORS, INCLUDING:

Annamaria Pahi
Columbia University
7 PUBLICATIONS **88** CITATIONS
SEE PROFILE

Zoltan Kiraly
University of Szeged
72 PUBLICATIONS **1,570** CITATIONS
SEE PROFILE

Ágnes Mastalir
University of Szeged
53 PUBLICATIONS **977** CITATIONS
SEE PROFILE

Available online at www.sciencedirect.com
ScienceDirect
Colloids and Surfaces A: Physicochem. Eng. Aspects 319 (2008) 77–83
COLLOIDS AND SURFACES A
www.elsevier.com/locate/colsurfa

Thermodynamics of micelle formation of the ephedrine-based chiral cationic surfactant DMEB in water, and the intercalation of DMEB in montmorillonite

Annamária B. Páhi [a], Dénes Varga [a], Zoltán Király [a,*], Ágnes Mastalir [b]

[a] *Department of Colloid Chemistry, University of Szeged, Aradi Vt. 1, H-6720 Szeged, Hungary*
[b] *Department of Organic Chemistry, University of Szeged, Dóm tér 8, H-6720 Szeged, Hungary*

Received 31 May 2007; received in revised form 27 June 2007; accepted 27 June 2007
Available online 30 June 2007

Abstract

The solubility and the micelle formation of the chiral cationic surfactant (1*R*,2*S*)-(−)-*N*-dodecyl-*N*-methylephedrinium bromide (DMEB) in aqueous solution were investigated by conductometry and titration microcalorimetry in the temperature range of 278–328 K. The Krafft temperature of DMEB is $T_K = 280$ K and the solubility of the surfactant at this point is 4.5 mM. The cmc versus T curve passes through a shallow minimum close to room temperature. The micelle formation changes from endothermic to exothermic at this characteristic temperature. The apparent degree of dissociation of the micelles α_{app} increases slightly as the temperature is raised. The isosteric enthalpies of micelle formation, $\Delta H_{st\,mic}$, are close to the calorimetrically measured enthalpies, ΔH_{mic}, provided that the real degree of dissociation, $\alpha_{st} = 1$, is used in the calculations. ΔH_{mic} and the temperature dependence of ΔH_{mic} of DMEB are markedly similar to those of sodium dodecylsulfate and dodecyltrimethylammonium bromide. The micelle formation of DMEB is favored by both enthalpy and entropy at and above room temperature. The enthalpy–entropy compensation results in a slight decrease in the Gibbs free energy on increase of the temperature. Sodium montmorillonite (M) was rendered organophilic by DMEB via ion-exchange to produce the clay/organocomplex DME-M. The swelling properties of the organoclay were investigated by XRD measurements in a variety of organic solvents. The basal spacing of DME-M varied from 1.8 to 3.5 nm, depending on the nature of the solvent. DME-M is a heterogenized ephedrine derivative, which may be regarded as a potential catalyst for enantioselective organic syntheses.

Keywords: Chiral surfactant; Conductometry; Microcalorimetry; Micelle; Montmorillonite

1. Introduction

Amphiphilic molecules possessing chemical or biochemical functionalities in their structures are called functional surfactants [1]. These compounds exhibit interesting surface-active properties, which cannot be achieved by their traditional counterparts. The synthesis and characterization of chiral surfactants have been intensively pursued because of their fundamental scientific and technological importance. The applications of chiral surfactants include the recognition of racemic compounds in the presence of chiral aggregates in solution [2,3], chromatographic and electrophoretic chiral separations of enantiomers [4–8], surfactant-templated syntheses of ordered chiral mesoporous sol–gel materials [9,10], and asymmetric catalysis for the synthesis of enantiomerically pure compounds [11–13].

Natural ephedrine (1*R*,2*S*)-(−)-α-(1-methylaminoethyl) benzyl alcohol, is a model molecule of β-aminoalcohols with two chiral centers in the molecule. (1*R*,2*S*)-(−)-*N*-dodecyl-*N*-methylephedrinium bromide (DMEB) consists of a hydrophobic dodecyl chain covalently bound to a positively charged ephedrine group with a quaternary ammonium nitrogen. The single-tailed cationic surfactant DMEB is a homolog of dodecyltrimethylammonium bromide (DTAB) and sodium dodecylsulfate (SDS), the prototypes of cationic and anionic surfactants, respectively (Fig. 1). DMEB has been applied as a chiral selector in capillary electrophoresis in order to separate a

* Corresponding author. Tel.: +36 62 544211; fax: +36 62 544042.
E-mail addresses: panna@chem.u-szeged.hu (A.B. Páhi), vargad@chem.u-szeged.hu (D. Varga), zkiraly@chem.u-szeged.hu (Z. Király), mastalir@chem.u-szeged.hu (Á. Mastalir).

0927-7757/$ – see front matter © 2007 Elsevier B.V. All rights reserved.
doi:10.1016/j.colsurfa.2007.06.056

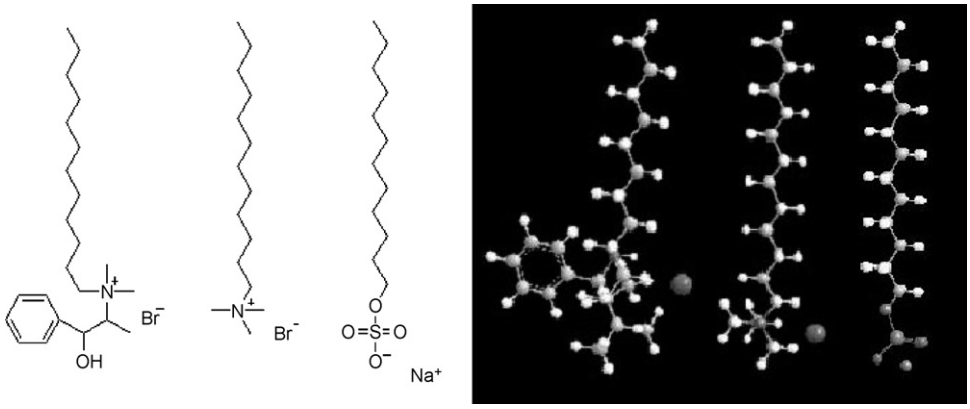

Fig. 1. The structure of (1*R*,2*S*)-(−)-*N*-dodecyl-*N*-methylephedrinium bromide (DMEB) as compared with the structures of dodecyltrimethylammonium bromide (DTAB) and sodium dodecylsulfate (SDS), prototypes of cationic and anionic surfactants, respectively.

variety of drug enantiomers [6,14,15]; as a surfactant template for the fabrication of enantioselective sol–gel thin films [16]; as a chiral phase transfer catalyst for asymmetric induction in the Michael reaction [17]; and as a micellar microenvironment for the synthesis of optically active α-amino acids [18]. Further, ephedrine derivatives have proved to be efficient catalysts in the enantioselective addition of diethylzinc to arylalkylaldehydes, under both homogenous [19,20] and heterogenous [21,22] reaction conditions. These examples imply the potential use of DMEB as a chiral catalyst in organic syntheses.

The micellar behavior of DMEB in aqueous solution has recently been investigated by means of surface tension measurements, conductometry, potentiometry and UV spectroscopy [23], and by surface tensiometry, fluorescence probe, light scattering and microscopic techniques [24]. The results of these studies are from certain important aspects contradictory. For instance, Oremusová and Greksáková reported that the hydrodynamic radius of DMEB aggregates at 303 K was 3.3 nm, which is consistent with the formation of spherical micelles [23]. In contrast, Roy et al. observed the formation of polydisperse giant vesicles at this temperature, with radii ranging from 165 nm to 1.1 μm [24].

We report here on the thermodynamics of the micelle formation of DMEB in aqueous solution, studied by conductometric titration and thermometric titration in the temperature range 278–328 K. In addition, the surfactant was immobilized in a cation-exchanger host material, montmorillonite (M), to give a clay/organocomplex dodecylmethylephedrinium montmorillonite (DME-M). The swelling properties (interlamellar expansion) of this ephedrine-based intercalation material were investigated by X-ray diffraction measurements in a variety of organic solvents.

2. Experimental

2.1. Materials

DMEB (purity: 99%) was purchased from Sigma–Aldrich and used as received. Water was percolated through ion-exchanger columns, followed by distillation, to give a specific conductance (κ) of 0.5–2.1 μS cm^{-1} in the temperature range studied. High-purity sodium montmorillonite EMX-826 was provided by Süd-Chemie AG (Germany). The nominal cation-exchange capacity of the clay was $CEC = 0.75$ mequiv g^{-1}.

2.2. Methods

2.2.1. Solution conductivity

Specific conductance measurements were performed in the temperature range 278–328 K with a PC-interfaced OK-114 conductometer (Radelkis, Hungary) equipped with an OK-0907P platinum electrode with sheet plates (cell constant $\kappa_{cell} = 1.02$ cm^{-1}). The measuring vessel was fitted with a magnetic stirrer and thermostated at $T \pm 0.05$ K. In a typical experiment, 25 mL of distilled water, or a dilute surfactant solution ($c <$ cmc) was titrated with 25 mL of a concentrated surfactant solution ($c >$ cmc) at 1-min intervals in aliquots of 0.5 mL by using a PC-controlled Titroline-96 volumetric titrator (Schott AG, Germany). The concentration of the titrant was less than 10 mM in order to eliminate incipient precipitation of the surfactant in the stock solution.

2.2.2. Titration microcalorimetry

Thermometric titration experiments were performed in the temperature range 288.15–328.15 ($\pm 2 \times 10^{-4}$) K with a Thermal Activity Monitor LKB-2277 isothermal heat-flow microcalorimeter (ThermoMetric, Sweden) [25]. A twin detector, supplied with a sample cell and a reference cell, was used. The sample cell was equipped with a stirring facility (60 rpm) and a Lund microtitrator. In a typical experiment, the calorimeter vessel was loaded with 2 mL of a dilute DMEB solution ($c <$ cmc), and 500 μL concentrated DMEB solution ($c >$ cmc) was injected into the vessel at 120-min intervals in aliquots of 20 μL. As for the conductometry, the concentration of the titrant was less than 10 mM in order to avoid the occurrence of precipitation in the titration syringe held outside the calorimeter at room temperature. The experiment was computer-controlled via DigiTam 4.1 software.

2.2.3. X-ray diffraction measurements

EMX-826 montmorillonite was rendered organophilic with DMEB via ion-exchange at 313 K [26]. The hydrophilic clay

was suspended in a concentrated aqueous solution of DMEB ($2 \times CEC$) and held at $T = 313$ K under stirring for 2 days. After organophilization, DME-M was purified by Soxhlet extraction in 2-propanol (48 h) and finally freeze-dried from benzene. The organic cation-exchange capacity was found to be $OCEC = 0.63 \pm 0.3$ mequiv g^{-1}, as determined with a Q-1500 D derivatograph (MOM, Hungary) and a TOC-1200 total organic content analyzer (Euroglass, Holland). The basal spacings (d_{001} reflections) of DME-M in suspensions were determined by using a Philips X-ray diffractometer (generator: PW 1830; goniometer: PW 1820; detector PW1711). Cu Kα radiation ($\lambda = 0.154$ nm) was applied at 40 kV and 35 mA. To prevent solvent evaporation, the samples were covered by a Mylar film.

3. Thermodynamic considerations

The variation of the cmc with temperature T can be approximated by a second-order polynomial [25,27–29]:

$$\ln \mathrm{CMC} = a + bT + cT^2 \quad (1)$$

Herein, CMC is the cmc expressed in mole fraction units; a, b and c are the fitting constants. In the multi-equilibrium model, the Gibbs free energy of micellization, ΔG_{mic}, of ionic surfactants can be expressed by [27–30]

$$\Delta G_{\mathrm{mic}} = RT(2-\alpha)\ln \mathrm{CMC} \quad (2)$$

where $0 \le \alpha \le 1$ is the degree of counterion dissociation of the micelle. α can be described by the polynomial expression [27–29]:

$$\alpha = a' + b'T + c'T^2 \quad (3)$$

At a constant external pressure P, the isosteric enthalpy of micelle formation, $\Delta H_{\mathrm{st\,mic}}$, can be calculated by means of the van't Hoff relation [25,27–30]:

$$\Delta H_{\mathrm{st\,mic}} = -RT^2\left((2-\alpha)\frac{\partial \ln \mathrm{CMC}}{\partial T} - \frac{\partial \alpha}{\partial T} \times \ln \mathrm{CMC}\right)_P$$
$$= -RT^2[(2-\alpha) \times (b + 2cT) - (b' + 2c'T) \times \ln \mathrm{CMC}] \approx a'' + b''T + c''T^2 \quad (4)$$

The entropy term, $T\Delta S_{\mathrm{mic}}$, and the heat capacity, $\Delta C_{p\,\mathrm{mic}}$, of micellization are given by

$$T\Delta S_{\mathrm{mic}} = \Delta H_{\mathrm{mic}} - \Delta G_{\mathrm{mic}} \quad (5)$$

$$\Delta C_{p\,\mathrm{mic}} = \left(\frac{\partial(\Delta H_{\mathrm{mic}})}{\partial T}\right)_P = b'' + 2c''T \quad (6)$$

The results of the calculation of the thermodynamic potential functions ΔX_{mic} via Eqs. (2), (4)–(6), depend critically on the value of α. This quantity can be determined experimentally by conductometric titration [23,28–31]. The exact meaning of α, however, is not straightforward. In a rigorous thermodynamic treatment, Gilányi criticized the use of α for making an arbitrary distinction between "free" and "bound" counterions [31]. In his terms, the experimentally measured degree of dissociation is an apparent quantity which has a value in the range $0 \le \alpha_{\mathrm{app}} \le 1$. This parameter reflects specific and long-range electrostatic interactions between the micelles and small ions. Excess counterions are distributed in the diffuse ionic atmosphere around the micelles. Gilányi argued that ionic micelles may be regarded as Stern particles which are fully dissociated, and that the true degree of dissociation is equal to, or at least close to unity: $\alpha_{\mathrm{st}} \approx 1$. With this choice of α, Eqs. (2) and (4) simplify to Eqs. (7) and (8), respectively:

$$\Delta G_{\mathrm{mic}} = RT \ln \mathrm{CMC}, \quad \alpha = 1 \quad (7)$$

$$\Delta H_{\mathrm{st\,mic}} = -RT^2\left(\frac{\partial \ln \mathrm{CMC}}{\partial T}\right)_P, \quad \alpha = 1 \quad (8)$$

These formulas are generally applied for non-ionic surfactants and frequently for ionic surfactants. In fact, in many instances, the best agreement between the calorimetric and the isosteric enthalpies can be achieved with the choice of $\alpha = 1$ [25,27–30]. It is of interest, therefore, to cross-check the isosteric enthalpies, $\Delta H_{\mathrm{st\,mic}}$, calculated by Eqs. (4) and (8) with ΔH_{mic} measured calorimetrically.

4. Results and discussion

4.1. Conductometric titration

DMEB displayed rather poor solubility in water. For stock solutions of $c > 12$ mM, the formation of needle-shaped crystals was observed upon storage at room temperature. The slow precipitation (lasting hours to days) was attributed to supersaturation of the parent solution; this observation motivated us to perform conductometric studies on both the solubility and the micelle formation of DMEB in water. Pure water or dilute DMEB solutions ($c < 4$ mM) were titrated with more concentrated surfactant solutions ($c \approx 10$ mM) below the saturation concentration ($c < c_{\mathrm{sat}}$) in order to avoid precipitation in the titration syringe held at room temperature. Fig. 2 depicts a series of the plots of specific conductance κ versus surfactant concentra-

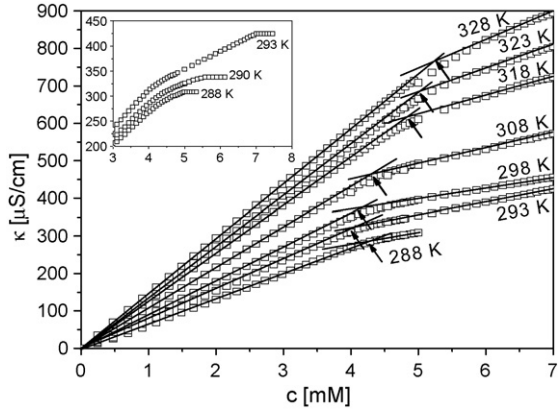

Fig. 2. Specific conductance of aqueous DMEB solutions plotted at different temperatures against the surfactant concentration. Titration curves in the insert: first break point ascribed to micelle formation; second break point ascribed to precipitation.

tion c in the range 288 K < T < 328 K. Each plot is linear with a change in slope S in the region of the cmc. The cmc was determined from the point of intersection of the two straight lines in the premicellar and the postmicellar regions. The conducting property of the charged micelles (Stern particles [31]) contrasted with the non-conducting property of the precipitate. In the range 280 K < T < 293 K and at 4.5 mM < c < 5.5 mM, two breaks appeared in the κ versus c curves (insert in Fig. 2). The first break was attributed to the cmc and the second one to c_{sat}. After saturation was reached, a constant or slightly decreasing conductance was measured with increasing c (insert in Fig. 2) due to the formation of an increasing number of non-conducting particles. Differentiation between c_{sat} and cmc was not straightforward at T < 288 K because of the closely spaced break points ascribed to micelle formation and precipitation, respectively. Nevertheless, phase separation was easily recognized by visual observation during the titration experiment: the transparent solution suddenly became turbid at $c = c_{sat}$. The phase diagram of DMEB in aqueous solution is given in Fig. 3. The c_{sat} versus T boundary was constructed by recording the compositions at which turbidity appeared. The cmc versus T diagram was constructed on the basis of both conductometric and thermometric titrations. The experimental data were fitted by using Eq. (1). The cmc passes through a shallow minimum at around room temperature. The intersection point of the c_{sat} versus T and the cmc versus T curves (the temperature at which c_{sat} = cmc) is situated at T = 280 K. This point is defined as the Krafft temperature, T_K [33–35]. At $T < T_K$, hydrated crystals are in equilibrium with surfactant monomers. At $T > T_K$, the solubility of DMEB increases rapidly and a micellar solution exists in the area surrounded by the solubility curve and the cmc curve (Fig. 3). Strictly, the Krafft point is not a single point, but extends over a narrow range of temperature because of the polydisperse nature of the micellar aggregates and the metastable nature of the solution in close vicinity to saturation [34,35]. T_K is a most important parameter of ionic surfactants. For instance, T_K is 298, 299 and 306 K for the common surfactants cetylpyridinium bromide, cetyltrimethylammonium bromide and sodium dodecylbenzenesulfonate, respectively [36], which makes these surfactants inconvenient for research or applications at room temperature.

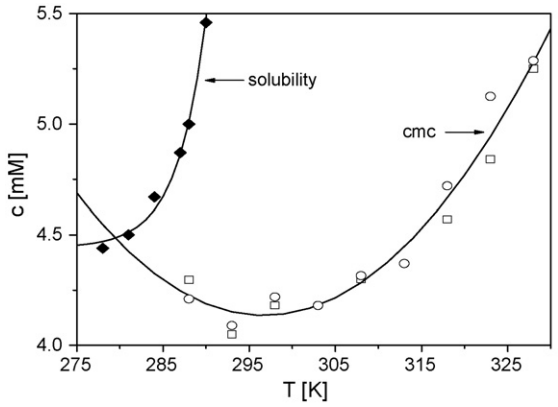

Fig. 3. Solubility and critical micelle concentration of DMEB in water as functions of temperature: (♦) and (□) conductometry; (◯) calorimetry.

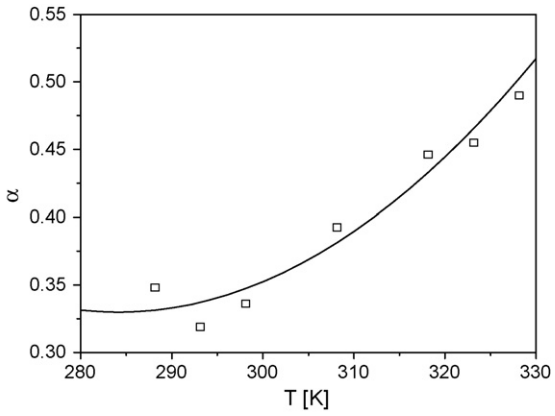

Fig. 4. The (apparent) degree of dissociation of DMEB micelles as a function of temperature.

The results of the conductometric measurements in Fig. 2 enabled us to calculate the (apparent) degree of dissociation α by taking the ratio of the slopes of the straight lines after (S_2) and before (S_1) the cmc: $\alpha = S_2/S_1$ [27–29,31]. Fig. 4 demonstrates that α increases from 0.33 to 0.49 as T is increased from 290 to 328 K. The experimental data were fitted by Eq. (3). The temperature dependence of α is similar to that reported by Oremusová and Greksáková [23], although the present α values are slightly higher. It has been suggested that for surfactant homologs having the same chain length but differing in the size of the head group, an increase in α is induced by an increased steric hindrance about the charged head, which in turn prevents the approach of the counterion to the head [32]; this explanation accounts for the slightly larger α of the bulky head group of DMEB as compared with those of DTAB or SDS.

4.2. Titration microcalorimetry

The differential enthalpies of dilution, ΔH_{dil}, at different temperatures are plotted against c in Fig. 5. The thermometric titration curves are sigmoidal in shape. In the premicellar region, ΔH_{dil} is mainly due to demicellization upon dilution of the titrant, although heats resulting from dilution of the resultant

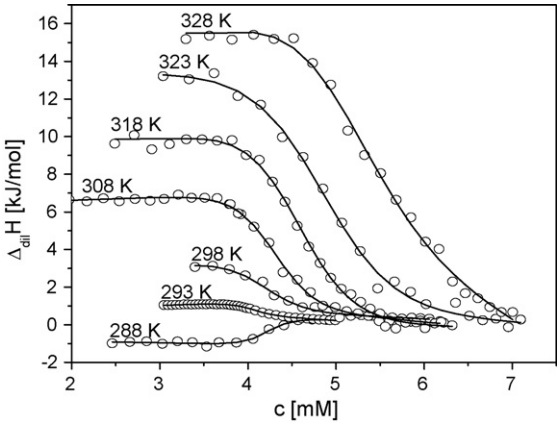

Fig. 5. Calorimetric enthalpies of dilution of micellar DMEB solutions (c > cmc) into dilute aqueous solutions (c < cmc) at different temperatures.

surfactant monomers and from dilution of the parent micelles are also included. ΔH_{dil} remains apparently constant until the enthalpy increases (or decreases, depending on the temperature) over a relatively narrow range of concentration. The cmc is situated in this transition region. As the cmc is approached and exceeded, fewer and fewer micelles decompose upon titration. Instead, the enthalpies of dilution of the micelles become increasingly dominant. In the third part of the sigmoidal curves, ΔH_{dil} shows little variation with c and the micelle dilution becomes close to athermal. For each titration curve, the cmc and ΔH_{mic} were evaluated by using a mathematical routine [25]:

$$\Delta H_{dil} = \frac{a_1 c + a_2}{1 + \exp(c - a_3)} + a_4 c + a_5 \quad (9)$$

where the a_i's are fitting parameters. The curve fitting yields the cmc at the inflection point (a_3 = cmc). This procedure provides essentially the same result when the position of the minimum (or the maximum, depending on the temperature) of the first derivative of the sigmoidal curve is regarded as the cmc. The enthalpy of micelle formation can be calculated from the height of the step function at the cmc, i.e. by taking the enthalpy difference between the two straight lines extrapolated to the cmc. At this position, $a_2 = \Delta H_{mic} = -\Delta H_{dil}$. Fig. 5 reveals that ΔH_{dil} changes sign from exothermic to endothermic somewhere between 288 and 293 K; at this inversion temperature, micelle decomposition is athermal in the entire range of surfactant concentration.

The calorimetric cmc values indicated in Fig. 3 are in good agreement with those determined by conductometry. Further, the present cmc versus T data agree well with those reported by Oremusová and Greksáková [23], but the two sets of data are significantly different from the results of Roy et al. [24]. These latter authors reported the occurrence of a micelle-to-vesicle transition at T = 301 K, and subsequent decomposition of the vesicles at T = 316.5 K [24]. The radius of the giant vesicles was found to be in the range 165 nm to 1.1 μm at 303 K. In contrast, Oremusová and Greksáková reported a micellar hydrodynamic radius of 3.3 nm at the same temperature, and no indication of vesicle formation was experienced in the temperature range studied (298–323 K). In general, calorimetry is a sensitive tool for the study of phase transition phenomena. The results of the present titration microcalorimetric study indicate that a micelle-to-vesicle transition is very unlikely to occur. However, since sphere-to-rod micellar transitions have been found to be nearly athermal [37,38], the occurrence of a micelle-to-vesicle transition for DMEB cannot be entirely excluded.

The calorimetric enthalpy data ΔH_{mic} are plotted as a function of temperature in Fig. 6

To a good approximation, the function is linear in the temperature range studied and has a negative slope. The enthalpy changes sign ($\Delta H_{mic} = 0$) at T = 292 K, close to the position of the minimum in the cmc versus T curve in Fig. 3. In fact, Eq. (8) predicts that micelle formation becomes athermal at a temperature when the cmc is minimum; $\Delta H_{st\,mic}$ is positive on the lower temperature side and negative on the higher temperature side of the minimum. Fig. 6 indicates that the agreement between $\Delta H_{st\,mic}$ (derived from the temperature dependence of the cmc) and ΔH_{mic} (directly measured by calorimetry) is satisfactory with the assumption of $\alpha = 1$ (Eq. (8)) although ΔH_{mic} is 2 kJ mol^{-1} more exothermic. The agreement is not satisfactory when $\alpha = \alpha(T)$ is applied in the calculations (Eq. (4)) and the disagreement increases with increasing temperature. This observation supports the abovementioned concept of Gilányi on α [31], and is in line with the experience of other researchers who found good agreement between the calorimetric and isosteric enthalpies with the choice of $\alpha = 1$ [25,27–30]. It should be emphasized that the directly measured calorimetric enthalpy data are free of assumptions and are therefore always more reliable than those calculated from the temperature dependence of the cmc and α.

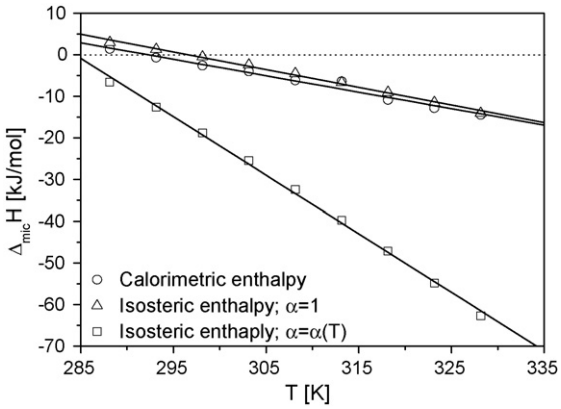

Fig. 6. Enthalpies of micelle formation of DMEB in aqueous solutions plotted against temperature. Comparison of the calorimetric enthalpies with the isosteric enthalpies calculated by Eq. (4) ($\alpha = \alpha(T)$) and Eq. (8) ($\alpha = 1$).

ΔH_{mic} versus T for DMEB is compared with those of DTAB [39] and SDS [40] in Fig. 7.

These compounds can be regarded as surfactant homologs of DMEB which possess the same alkyl chain length but different ionic head groups (Fig. 1). The relationship between ΔH_{mic} and T is markedly linear and the data lie on essentially the same straight line, regardless of the nature of the ionic head. Linear regression analysis yields $\Delta C_{p\,mic} = -420$ J K^{-1} mol^{-1} for the molar heat capacity of micellization of DMEB in water

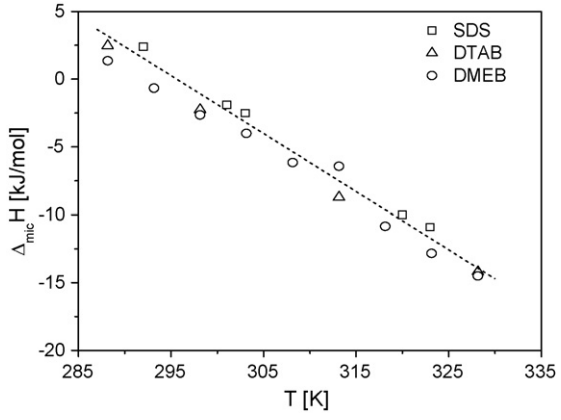

Fig. 7. Calorimetric enthalpies of micelle formation of DMEB (this work), dodecyltrimethylammonium bromide DTAB [39] and sodium dodecylsulfate SDS [40] in aqueous solutions as functions of temperature.

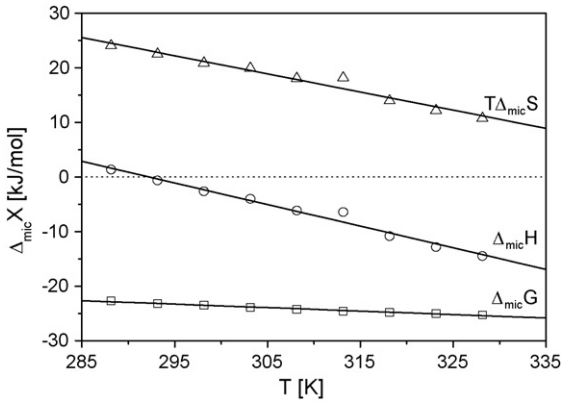

Fig. 8. Enthalpy, Gibbs free energy and entropy terms of the micelle formation of DMEB in aqueous solution (calorimetric data in combination with Eqs. (5) and (7)).

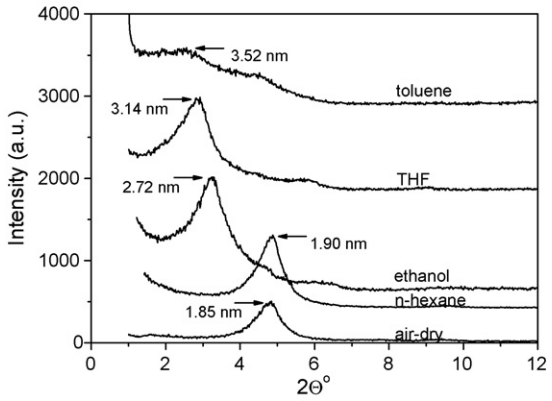

Fig. 9. XRD patterns of DME-montmorillonite in the air-dry state and dispersed in various organic liquids.

(Eq. (6); $c'' = 0$) as compared with $\Delta C_{p\,\mathrm{mic}} = -423\,\mathrm{J\,K^{-1}\,mol^{-1}}$ for DTAB [39] and $\Delta C_{p\,\mathrm{mic}} = -426\,\mathrm{J\,K^{-1}\,mol^{-1}}$ for SDS [40]. The similarity of these values implies that, for ionic surfactants, ΔH_{mic} and temperature dependence of ΔH_{mic} are influenced less by the nature of the head group than by the length of the alkyl chain ($-\Delta C_{p\,\mathrm{mic}}$ is about $50\,\mathrm{J\,K^{-1}\,mol^{-1}}$ for a –CH_2– segment [25,30,39,40]).

The thermodynamic potential functions of micelle formation, ΔH_{mic}, ΔG_{mic} and $T\Delta S_{\mathrm{mic}}$, are given in Fig. 8. To a good approximation, the variations of these quantities with T are linear in the temperature range studied. Before the micelle formation changes from endothermic to exothermic, the process is entropically driven and opposed by enthalpy, after which both the enthalpy and the entropy terms favor micellization. Fig. 8 illustrates well the delicate balance between the change in enthalpy and the change in entropy as the temperature is raised: large changes in the two quantities result in a moderate decrease in the Gibbs free energy (enthalpy/entropy compensation).

At a molecular level, micelle formation is promoted by van der Waals interactions between the alkyl chains of the amphiphilic molecules (favored by enthalpy) and the concominant release of structured hydration water into the bulk (favored by entropy). The extensive hydrogen bonding in water gradually breaks down with increasing temperature, the importance of the entropic term of hydrophobic hydration therefore decreases, and the dispersion interactions become increasingly dominant [41,42]. Coulombic repulsion between neighboring ionic heads, Coulombic attraction between the ionic heads and the counterions, and the associated changes in head group hydration should also be considered in the overall micellization process [25,27–30,40,42]. However, it is difficult to separate the contributions of the various subprocesses, and such an analysis is beyond the scope of the present study.

4.3. X-ray diffraction measurements on DME-M

The XRD patterns of DME-M in the air-dry state, and dispersed in various organic liquids (*n*-hexane, ethanol, tetrahydrofuran (THF) and toluene) are given in Fig. 9. The basal spacings d_{001} of the clay/organocomplex were calculated from the positions of the peak maxima corresponding to the first-order Bragg reflections. d_{001} increases in the sequence of 1.85, 1.90, 2.72, 3.14 and 3.52 nm, corresponding to the air-dry state, *n*-hexane, ethanol, THF and toluene, respectively. For the dry organoclay, the alkyl chains lie flat on the surface of the montmorillonite host and hold the aluminosilicate layers apart permanently. The basal spacing is equal to the thickness of the silicate layer plus twice the cross-section of the organic cation [26,43,44]. The extent of swelling of the organoclay is negligible in *n*-hexane, suggesting that this nonpolar solvent cannot penetrate the interlamellar space. The pronounced interlayer expansion in ethanol, THF and toluene is attributed to the efficient wetting of the silicate surface and/or the good solvation of the alkyl chains by these solvents. Under these conditions, the alkyl chains are lifted away from the solid surface to form an interdigitated bilayer in which the chains are tilted or oriented vertically to the surface [26,43,44]. The sharp peaks in Fig. 9 originate from highly ordered lamella packages in the dispersion liquids with the exception of toluene. Although d_{001} is largest in toluene, the reflection is of low intensity and rather diffuse, which indicates that swelling is accompanied by a pronounced delamination. The occurrence of exfoliation, when the individual montmorillonite platelets no longer exhibit an XRD deflection, can be excluded. Delamination of the clay lamella packages is often accompanied by the formation of an open card-house structure (edge-to-face flocculation), leading to the appearance of thixotropic behavior [45,46]. Visual observation provided evidence of a high degree of thixotropy of DME-M in toluene; complete space filling (gelation) occurred even in dilute suspensions, which readily transformed to a low-viscosity fluid when shaken gently, and then became semisolid again upon standing.

The swelling of organoclays permits ready access to the gallery sheets which are important in many applications, e.g. metal particle synthesis in nanophase reactors [47,48], intercalation catalysis [47–49] or adsolubilization [44,50,51]. As mentioned in the Introduction, ephedrine proved to be an efficient catalyst in the enantioselective alkylation of aldehydes by diethylzinc in toluene solution [19–22]. DMEB is currently being investigated in related reactions; our preliminary results

indicated that this chiral surfactant is active and selective under both homogenous and heterogenous conditions.

4.4. Conclusions

DMEB in aqueous solution has a Krafft temperature $T_K = 280\,K$ and a solubility $c_{sat} = 4.5\,mM$ at the T_K. The cmc versus T plot passes through a shallow minimum at around room temperature, where the micelle formation changes from endothermic to exothermic. Above this temperature, micelle formation is promoted by both enthalpy and entropy. The apparent degree of dissociation α_{app} increases with increasing T. The agreement between the isosteric enthalpies $\Delta H_{st\,mic}$ and the calorimetric enthalpies ΔH_{mic} is satisfactory when the real degree of dissociation, $\alpha_{st} = 1$ is applied in the thermodynamic formulations. The Gibbs free energy, ΔG_{mic}, decreases only slightly with increasing T due to enthalpy–entropy compensation. Sodium montmorillonite was rendered organophilic by DMEB. The organoclay undergoes swelling in a variety of organic solvents. The extent of interlayer expansion depends on the nature of the solvent. DME-M is a heterogenized ephedrine derivative which may find applications in enantioselective catalysis.

Acknowledgments

This work was supported by the Bolyai János Foundation and the Hungarian Scientific Research Fund (OTKA T047390 and OTKA T068152).

References

[1] Y.-Y. Luk, N.L. Abbott, Curr. Opin. Colloid Interface Sci. 7 (2002) 267.
[2] J. Bella, S. Borocci, G. Mancini, Langmuir 15 (1999) 8025.
[3] F. Ceccacci, M. Diociaiuti, L. Galantini, G. Mancini, P. Mencarelli, A. Scipioni, C. Villani, Org. Lett. 6 (2004) 1565.
[4] S. Terabe, K. Otsuka, K. Ichikawa, A. Tsuchiya, T. Ando, Anal. Chem. 56 (1984) 111.
[5] A. Dobashi, T. Ono, S. Hara, J. Yamaguchi, J. Chromatogr. 480 (1989) 413.
[6] G. Gübitz, M.G. Schmid, Electrophoresis 21 (2000) 4112.
[7] J. Tarus, A.A. Shamsi, K. Morris, R.A. Agbaria, I.M. Warner, Langmuir 19 (2003) 7173.
[8] K. Kurata, J. Ono, A. Dobashi, J. Chromatogr. A 1080 (2005) 140.
[9] S. Che, Z. Liu, T. Ohsuna, K. Sakamoto, O. Terasaki, T. Tatsumi, Nature 429 (2004) 281.
[10] S. Che, J. Nanosci. Nanotech. 6 (2006) 1557.
[11] H.J. Li, H.Y. Tian, Y.J. Chen, D. Wang, C.J. Li, J. Chem. Res. 3 (2003) 153.
[12] T.A. Davidson, K. Mondal, X. Yang, J. Colloid Interface Sci. 276 (2004) 498.
[13] S. Roy, D. Das, A. Dasgupta, R.N. Mitra, P.K. Das, Langmuir 21 (2005) 10398.
[14] A. Bunke, Th. Jira, Th. Beyrich, Pharmazie 52 (1997) 762.
[15] S. Roy, D. Khatua, J. Chromatogr. A 1048 (2004) 127.
[16] S. Fireman-Shores, I. Popov, I.D. Avnir, S. Marx, J. Am. Chem. Soc. 127 (2005) 2650.
[17] S. Colonna, A. Re, J. Chem. Soc., Perkin I (1981) 547.
[18] W. Wu, Y. Zhang, Tetrahedron Asymmetry 9 (1998) 1441.
[19] P.A. Chaloner, S.A.R. Perera, Tetrahedron Lett. 28 (1987) 3013.
[20] J. Näslund, C.J. Welch, Tetrahedron Asymmetry 2 (1991) 1123.
[21] D.W.L. Sung, P. Hodge, P.W. Stratford, J. Chem. Soc., Perkin Trans. I (1999) 1463.
[22] S. Abramson, M. Laspéras, A. Galarneau, D. Desplantier-Giscard, D. Brunel, Chem. Commun. (2000) 1773.
[23] J. Oremusová, O. Greksáková, Tenside Surf. Det. 40 (2003) 90.
[24] S. Roy, D. Khatua, J. Dey, J. Colloid Interface Sci. 292 (2005) 255.
[25] Z. Király, I. Dékány, J. Colloid Interface Sci. 242 (2001) 214.
[26] I. Dékány, F. Szántó, L.G. Nagy, J. Colloid Interface Sci. 109 (1986) 376.
[27] J.J.H. Nusselder, J.B.F.N. Engberts, J. Colloid Interface Sci. 148 (1992) 353.
[28] A. Chatterjee, S.P. Moulik, S.K. Sanyal, B.K. Mishra, P.N. Puri, J. Phys. Chem. B 105 (2001) 12823.
[29] G.B. Ray, I. Chakraborty, S. Ghosh, S.P. Moulik, R. Palepu, Langmuir 21 (2005) 10958.
[30] S. Shimizu, R.P. Paulo Augusto, O.A. El Soud, Langmuir 20 (2004) 9551.
[31] T. Gilányi, J. Colloid Interface Sci. 125 (1988) 641.
[32] R. Zana, J. Colloid Interface Sci. 78 (1980) 330.
[33] D.N. Eggenberger, H.J. Harwood, J. Am. Chem. Soc. 73 (1951) 3353.
[34] Y. Moroi, R. Matura, Bull. Chem. Soc. Jpn. 61 (1988) 333.
[35] T.W. Davey, W.A. Ducker, A.R. Hayman, J. Simpson, Langmuir 14 (1998) 3210.
[36] N.M. Van Os, J.R. Haak, L.A.M. Rupert, Physico-Chemical Properties of Selected Anionic, Cationic and Nonionic Surfactants, Elsevier, Amsterdam, 1993.
[37] P.J. Missel, N.A. Mazer, G.B. Benedek, C.Y. Young, M.C. Carey, J. Phys. Chem. 84 (1980) 1044.
[38] N.A. Mazer, G. Olofsson, J. Phys. Chem. 86 (1982) 4584.
[39] M.T. Bashford, E.M. Woolley, J. Phys. Chem. 89 (1985) 3173.
[40] S. Paula, W. Süs, J. Tuchtenhagen, A. Blume, J. Phys. Chem. 99 (1995) 11742.
[41] C. Tanford, The Hydrophobic Effect: Formation of Micelles and Biological Membranes, Wiley, New York, 1980.
[42] W. Blokzijl, J.B.F.N. Engberts, Angew. Chem. Int. Ed. Engl. 32 (1993) 1545.
[43] I. Dékány, F. Szántó, A. Weiss, G. Lagaly, Ber. Bunsen. Phys. Chem. 90 (1986) 427.
[44] I. Dékány, A. Farkas, Z. Király, E. Klumpp, H.D. Narres, Colloids Surf. 119 (1996) 7.
[45] T.R. Jones, Clay Miner. 18 (1983) 399.
[46] J. Li, J.P. Oberhauser, J. Rheol. 50 (2006) 729.
[47] Z. Király, I. Dékány, Á. Mastalir, M. Bartók, J. Catal. 161 (1996) 401.
[48] Á. Mastalir, F. Notheisz, Z. Király, M. Bartók, I. Dékány, Stud. Surf. Sci. Catal. 108 (1997) 477.
[49] Z. Király, B. Veisz, Á. Mastalir, G. Kőfaragó, Langmuir 17 (2001) 5381.
[50] L.P. Meier, R. Nueesch, F.T. Madsen, J. Colloid Interface Sci. 238 (2001) 24.
[51] B. Witthuhn, T. Pernyeszi, P. Klauth, H. Vereecken, E. Klumpp, Colloids Surf. A 265 (2005) 81.